

UC Davis

UC Davis Previously Published Works

Title

Characterizing low fluence thresholds for in vitro photodynamic therapy

Permalink

<https://escholarship.org/uc/item/0f68990f>

Journal

Biomedical Optics Express, 6(3)

ISSN

2156-7085

Authors

Hartl, Brad A
Hirschberg, Henry
Marcu, Laura
et al.

Publication Date

2015-03-01

DOI

10.1364/boe.6.000770

Peer reviewed

Characterizing low fluence thresholds for *in vitro* photodynamic therapy

Brad A. Hartl,^{1,*} Henry Hirschberg,² Laura Marcu,¹ and Simon R. Cherry¹

¹ Department of Biomedical Engineering, University of California, Davis, Davis, CA 95616, USA

² Beckman Laser Institute and Medical Clinic, University of California, Irvine, Irvine, CA 92697, USA

*bahartl@ucdavis.edu

Abstract: The translation of photodynamic therapy (PDT) to the clinic has mostly been limited to superficial diseases where traditional light delivery is noninvasive. To overcome this limitation, a variety of mechanisms have been suggested to noninvasively deliver light to deep tissues. This work explores the minimum amount of light required by these methods to produce a meaningful PDT effect in the *in vitro* setting under representative low fluence and wavelength conditions. This threshold was found to be around 192 mJ/cm² using the clinically approved photosensitizer aminolevulinic acid and 12 mJ/cm² for the more efficient, second generation photosensitizer TPPS_{2a}.

©2015 Optical Society of America

OCIS codes: (170.5180) Photodynamic therapy; (170.0170) Medical optics and biotechnology.

References and links

1. P. Agostinis, K. Berg, K. A. Cengel, T. H. Foster, A. W. Girotti, S. O. Gollnick, S. M. Hahn, M. R. Hamblin, A. Juzeniene, D. Kessel, M. Korbelik, J. Moan, P. Mroz, D. Nowis, J. Piette, B. C. Wilson, and J. Golab, "Photodynamic therapy of cancer: an update," *CA Cancer J. Clin.* **61**(4), 250–281 (2011).
2. P. Babilas, S. Schreml, M. Landthaler, and R. M. Szeimies, "Photodynamic therapy in dermatology: state-of-the-art," *Photodermatol. Photoimmunol. Photomed.* **26**(3), 118–132 (2010).
3. S. Michels and U. Schmidt-Erfurth, "Photodynamic therapy with verteporfin: a new treatment in ophthalmology," *Semin. Ophthalmol.* **16**(4), 201–206 (2001).
4. J. N. Silva, P. Filipe, P. Morlière, J. C. Mazière, J. P. Freitas, M. M. Gomes, and R. Santus, "Photodynamic therapy: Dermatology and ophthalmology as main fields of current applications in clinic," *Biomed. Mater. Eng.* **18**(4-5), 319–327 (2008).
5. L. Costa, M. A. Faustino, M. G. Neves, A. Cunha, and A. Almeida, "Photodynamic inactivation of mammalian viruses and bacteriophages," *Viruses* **4**(12), 1034–1074 (2012).
6. P. Calzavara-Pinton, M. T. Rossi, R. Sala, and M. Venturini, "Photodynamic antifungal chemotherapy," *Photochem. Photobiol.* **88**(3), 512–522 (2012).
7. Z. Huang, H. Xu, A. D. Meyers, A. I. Musani, L. Wang, R. Tagg, A. B. Barqawi, and Y. K. Chen, "Photodynamic therapy for treatment of solid tumors—potential and technical challenges," *Technol. Cancer Res. Treat.* **7**(4), 309–320 (2008).
8. Y. D. Hu, K. Wang, and T. C. Zhu, "A light blanket for intraoperative photodynamic therapy," *Proc. SPIE* **7380**, 73801W (2009).
9. M. S. Mathews, E. Angell-Petersen, R. Sanchez, C. H. Sun, V. Vo, H. Hirschberg, and S. J. Madsen, "The effects of ultra low fluence rate single and repetitive photodynamic therapy on glioma spheroids," *Lasers Surg. Med.* **41**(8), 578–584 (2009).
10. B. C. Wilson and M. S. Patterson, "The physics, biophysics and technology of photodynamic therapy," *Phys. Med. Biol.* **53**(9), R61–R109 (2008).
11. B. W. Henderson, T. M. Busch, and J. W. Snyder, "Fluence rate as a modulator of PDT mechanisms," *Lasers Surg. Med.* **38**(5), 489–493 (2006).
12. S. K. Bisland, L. Lilge, A. Lin, R. Rusnov, and B. C. Wilson, "Metronomic photodynamic therapy as a new paradigm for photodynamic therapy: rationale and preclinical evaluation of technical feasibility for treating malignant brain tumors," *Photochem. Photobiol.* **80**(1), 22–30 (2004).
13. W. Chen and J. Zhang, "Using Nanoparticles to Enable Simultaneous Radiation and Photodynamic Therapies for Cancer Treatment," *J. Nanosci. Nanotechnol.* **6**(4), 1159–1166 (2006).
14. X. Zou, M. Yao, L. Ma, M. Hossu, X. Han, P. Juzenas, and W. Chen, "X-ray-induced nanoparticle-based photodynamic therapy of cancer," *Nanomedicine (Lond)* **9**(15), 2339–2351 (2014).
15. M. Haase and H. Schäfer, "Upconverting Nanoparticles," *Angew. Chem. Int. Ed. Engl.* **50**(26), 5808–5829 (2011).

16. N. M. Idris, M. K. Gnanasamandhan, J. Zhang, P. C. Ho, R. Mahendran, and Y. Zhang, "In vivo photodynamic therapy using upconversion nanoparticles as remote-controlled nanotransducers," *Nat. Med.* **18**(10), 1580–1585 (2012).
17. R. Laptev, M. Nisnevitch, G. Siboni, Z. Malik, and M. A. Firer, "Intracellular chemiluminescence activates targeted photodynamic destruction of leukaemic cells," *Br. J. Cancer* **95**(2), 189–196 (2006).
18. R. Robertson, M. S. Germanos, C. Li, G. S. Mitchell, S. R. Cherry, and M. D. Silva, "Optical imaging of Cerenkov light generation from positron-emitting radiotracers," *Phys. Med. Biol.* **54**(16), N355–N365 (2009).
19. J. Gonzales, G. Zamora, A. Trinidad, L. Marcu, S. Cherry, and H. Hirschberg, "Ultra low fluence rate photodynamic therapy: Simulation of light emitted by the Cerenkov effect," in (SPIE Proceedings, 2014), 89280F.
20. T. Hatakeyama, Y. Murayama, S. Komatsu, A. Shiozaki, Y. Kuriu, H. Ikoma, M. Nakanishi, D. Ichikawa, H. Fujiwara, K. Okamoto, T. Ochiai, Y. Kokuba, K. Inoue, M. Nakajima, and E. Otsuji, "Efficacy of 5-aminolevulinic acid-mediated photodynamic therapy using light-emitting diodes in human colon cancer cells," *Oncol. Rep.* **29**(3), 911–916 (2013).
21. S. Sharma, A. Jajoo, and A. Dube, "5-Aminolevulinic acid-induced protoporphyrin-IX accumulation and associated phototoxicity in macrophages and oral cancer cell lines," *J. Photochem. Photobiol. B* **88**(2-3), 156–162 (2007).
22. SciDAVis, retrieved December 2014, <http://scidavis.sourceforge.net/>.
23. B. F. Godley, F. A. Shamsi, F. Q. Liang, S. G. Jarrett, S. Davies, and M. Boulton, "Blue light induces mitochondrial DNA damage and free radical production in epithelial cells," *J. Biol. Chem.* **280**(22), 21061–21066 (2005).
24. T. Takahashi and T. Ogura, "Resonance Raman spectra of cytochrome c oxidase in whole mitochondria," *Bull. Chem. Soc. Jpn.* **75**(5), 1001–1004 (2002).
25. J. Zhang, K. L. Wong, W. K. Wong, N. K. Mak, D. W. Kwong, and H. L. Tam, "Two-photon induced luminescence, singlet oxygen generation, cellular uptake and photocytotoxic properties of amphiphilic Ru(II) polypyridyl-porphyrin conjugates as potential bifunctional photodynamic therapeutic agents," *Org. Biomol. Chem.* **9**(17), 6004–6010 (2011).

1. Introduction

Photodynamic therapy (PDT) is a type of medical treatment which uses light and photosensitizers to generate reactive oxygen species which destroy targeted cells and tissues. With an extensive array of photosensitizers to choose from, PDT has been studied as a treatment for a wide variety of tumors [1], skin diseases [2], macular degeneration [3, 4], as well as viral [5], bacterial [5], and fungal [6] infections. Despite these successes, PDT has only been FDA approved for a select few diseases, all of which are located superficially and can be accessed noninvasively. This is largely due to the difficulties associated with delivering light to deeper tissues using traditional light sources. The two most common light sources used to activate the photosensitizers are lasers and light emitting diodes (LEDs). The goal for all illumination sources is to deliver a homogeneous dose to all of the photosensitizer in the targeted tissue. For superficial and deep sites, a variety of methods to accomplish this have been implemented. Lasers are coupled into an optical fiber and can use either a microlens array or diffuser to deliver the light homogeneously [7], and to cover a larger area light blankets using side-glowing fibers have also been studied [8]. Alternatively, LEDs can be mounted in a planar array or in a customizable geometry to best fit the targeted region. Regardless of the location, the longest wavelength possible for the chosen photosensitizer is typically used in order to deliver light to as deep below the accessible surface as possible. However, due to the absorption of light in tissue, this inherently provides a gradient of light doses across the different depths.

For both superficial and deep illumination in the clinical setting there is a limited amount of time available to deliver the light. For superficial treatments this is primarily for patient convenience, and for deep surgical sites this is due to obvious difficulties associated with maintaining an implant inside a sterile cavity for extended periods of time. To accommodate the limited available time, high fluence rates are often used, despite it being known that the use of these fluence rates is less efficient [9]. This loss of efficiency is primarily caused by oxygen depletion in tissues which leads to photobleaching of the available photosensitizers [10]. This issue can be further exacerbated in the hypoxic regions of tumors where the available oxygen is even less. The fluence rate has also been shown to have an effect on the

mechanism of cell death in PDT [11], which can include direct cell damage (apoptosis and/or necrosis), vascular damage, and activation of an immune response. The use of low fluence rates has notably been shown to cause increased selective apoptosis (programmed cell death) of tumor cells [12], which is more desirable when compared to the inflammation and edema that commonly occur with the uncontrolled rupturing of cellular contents of necrosis.

To overcome the depth limitations of traditionally illuminated PDT and take advantage of the benefits from low fluence rates, a variety of noninvasive deep light sources have been proposed. Perhaps the most studied of these methods are scintillating nanoparticles which emit visible light when exposed to x-rays or gamma rays from an adjunctive therapy [13]. Positive results have been seen *in vitro* [14] though this method has yet to be tested *in vivo*. Upconverting nanoparticles use similar principles but instead use near infrared as the activation source instead of x-rays [15]. These nanoparticles convert the longer wavelength light into shorter wavelengths that can be used to activate photosensitizers. Although positive results have been seen *in vivo* [16], they will ultimately still be limited by the penetration depth of the near infrared light. Chemiluminescence utilizes chemical reactions to produce light and has been demonstrated to activate PDT *in vitro* [17]. However, finding chemicals that can be used in the *in vivo* setting still remains a significant challenge. Cerenkov luminescence is a small amount of ultraviolet and visible light that is generated from high-energy charged particles, such as those emitted from many radionuclides used for imaging and therapy. It has mostly been used for small animal imaging [18] thus far, but also has been suggested as possible means to excite photosensitizers deep within the body [19]. Cerenkov luminescence would be particularly well suited for deep illumination of PDT due to the availability of numerous clinically approved radiopharmaceuticals.

Compared to traditional clinical light sources these noninvasive deep light sources produce light at shorter wavelengths and at much lower intensities. Whereas traditionally in PDT greater light penetration from longer wavelengths is beneficial, due to these methods' ability to localize and generate light at the cellular level, less light propagation from the shorter wavelengths can provide improved light dose localization. These properties could then be used to compensate for a less specific photosensitizer and also allows metastatic sites to receive light doses which might have been missed with traditional external illumination. It is also important to note that most photosensitizers, and especially porphyrin-based ones, have much stronger and broader absorption at shorter wavelengths which provides further benefits of using noninvasive deep light sources.

For most of these noninvasive deep light sources the goal is not necessarily to provide a standalone PDT treatment for a disease, but rather an additional therapy that could ideally produce a synergistic effect when combined with another treatment, such as radiotherapy, brachytherapy, and/or chemotherapy. This work therefore aims to characterize and quantify the effectiveness of PDT in the *in vitro* setting to establish approximate light thresholds to serve as guidance for therapeutic light levels based on noninvasive deep light sources. Firstly, this paper compares excitation using blue and red LEDs to investigate if there is any intrinsic benefit from activating photosensitizers using the shorter wavelengths commonly emitted by noninvasive deep light sources. For these studies the clinically approved photosensitizer aminolevulinic acid (ALA) is used. Secondly, an approximate low fluence threshold for *in vitro* PDT was determined using the second generation photosensitizer TPPS_{2a}. Although even more efficient photosensitizers are being developed, TPPS_{2a} is commercially available. In order to generate illumination conditions representative of the noninvasive deep light sources as well as traditional ones, a custom light source was developed to deliver light at a wide range of fluence rates over extended periods of time without perturbing cell culture conditions. This light source was then used to generate fluence dose-response curves for *in vitro* PDT of three different tumor cell lines. This paper explores the lower limit of light doses that are needed to produce a meaningful effect from photodynamic therapy in the *in vitro* setting.

2. Methods

2.1 Cell culture

Three different cancer cell lines were chosen in order to study and compare a variety of deep tumor tissue types that could be treated using photodynamic therapy and noninvasive deep light sources. The U-87 MG glioblastoma and A-498 renal carcinoma cell lines (purchased through the American Type Culture Collection) were cultured at 37° C and 5% CO₂ in Dulbecco's Eagle's Minimum Essential Medium (Gibco, Grand Island, NY) without phenol red indicator and with 10% fetal bovine serum (FBS), penicillin (100 U/ml) and streptomycin (100 µg/ml). The MDA-MB-231-luc-D3H1 breast tumor cell line (purchased from Perkin Elmer Inc., Waltham, MA) was cultured under the same conditions.

2.2 LED illumination

In order to provide a wide range of fluence rates over extended periods of time for *in vitro* PDT studies, a custom LED illumination source (Fig. 1(a),1(b)) was developed. Surface mount LEDs with peak and full width at half maximum wavelengths of 405/14 nm and 634/14 nm (VLMU3100-GS08 and VLMS33S1U1-GS08, Vishay Intertechnology Inc., Malvern, PA) were mounted on a printed circuit board (PCB). These LEDs were chosen to match the Soret- and Q-band absorption peaks of the photosensitizer protoporphyrin IX (PpIX, produced by the prodrug ALA) as seen in Fig. 1(c) and therefore represent optimal excitation conditions for both traditional and noninvasive deep light sources. For absorption spectral measurements PpIX and TPPS_{2a} were dissolved in DMSO and data recorded using a UV-Vis spectrophotometer (Cary 300, Varian Inc., Palo Alto, CA). A total of 60 red or blue LEDs were soldered on each board such that they were located directly above the center of each well of a white, clear bottom 96-well plate. To achieve precise control over the current driving the LEDs, 12-channel constant-current sink drivers (TLC5971, Texas Instruments Inc., Dallas, TX) were employed. This setup thus provides six fluence rates per plate, allowing for five treatment wells and five light-only controls per group. Each driver and its 12 channels were controlled with an Arduino Uno microcontroller board (Smart Projects, Italy). This provides vastly more flexibility of fluence rates compared to commonly used methods, which rely on physical neutral density filters to provide different fluence rates [20].

Fluence rates reported herein were corrected for overhead illumination geometry, including attenuation at corresponding wavelengths due to the cell culture media and photosensitizer. These correction factors were further validated by comparing the results from *in vitro* PDT studies using the LED setup with those performed using a traditional bottom-illumination configuration with clear plates and a laser. For these comparative studies, a 405 nm laser (CUBE 405-50, Coherent Inc., Santa Clara, CA) fiber-optically coupled to an engineered diffuser (ED1-S50-MD, Thorlabs Inc., Newton, NJ) was used. Fluence rates and spectra were measured with an optical power meter (PM100D power meter, S120VC power sensor, Thorlabs Inc., Newton, NJ) and spectrophotometer (USB2000 Miniature Fiber Optic Spectrometer, Ocean Optics Inc., Dunedin, FL), respectively. Due to the extremely low fluence rates used in the experiments, it was necessary to make measurements below the power meter's specified range. For these ultra-low measurements, however, the power meter's accuracy was verified with the use of calibrated neutral density filters. Black hardboard (Thorlabs Inc., Newton, NJ) was placed one centimeter below the bottom of the multi-well plates in order to prevent reflection of light back into the wells. To demonstrate the range of fluence rates that these illumination sources are capable of delivering, their average fluence rates have been plotted in Fig. 1(d). No increases in temperature were detected from the use of the LED array at the fluence rates used herein for *in vitro* PDT studies.

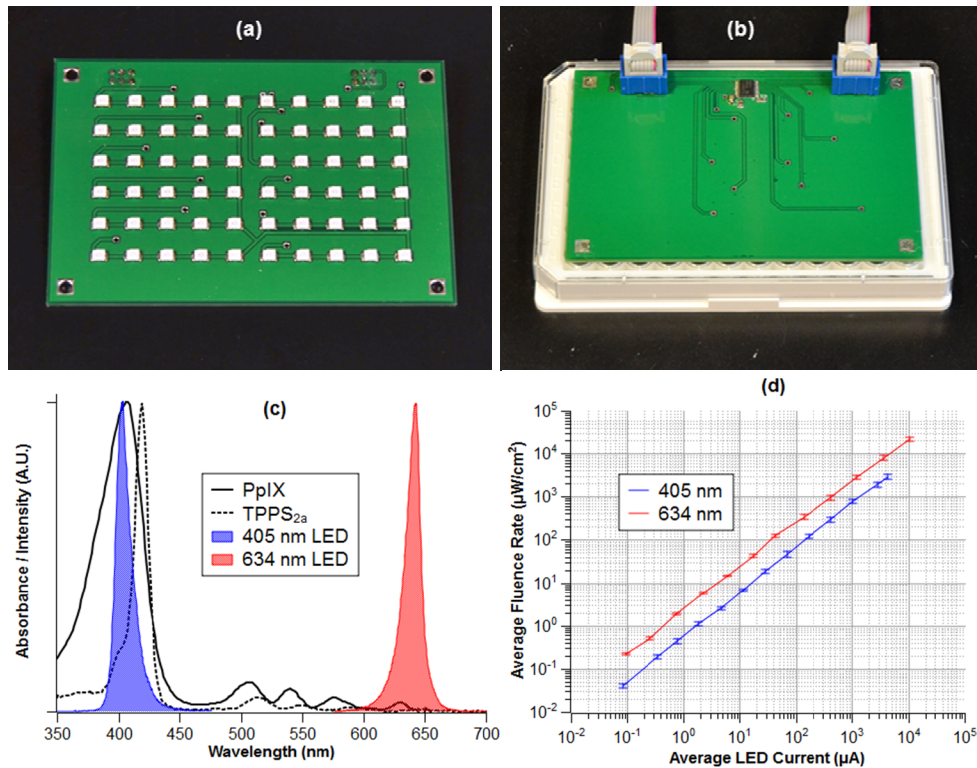


Fig. 1. Setup and characterization of LED illumination source: Bottom of PCB with LEDs (a), setup for *in vitro* PDT studies with PCB attached to transparent 96-well plate lid (b), normalized absorption spectra for PpIX and TPPS_{2a} in DMSO, and emission spectra for the 405 nm and 634 nm LEDs (c), the dynamic range of the fluence rates that can be generated from each type of LED (d).

2.3 PDT treatments

Cells were seeded with 100 μl/well of media on white, clear bottom 96-well plates at 2×10^3 cells/well. For ALA studies cells were incubated at 1 mM ALA (Sigma-Aldrich Co., St. Louis, MO) for 6 hours with media containing a reduced FBS concentration of 2%. A reduction in FBS concentration was used, as serum is well known to reduce intracellular PpIX accumulation and therefore decrease the efficiency of PDT [21]. For studies using TPPS_{2a} (Frontier Scientific Inc., Logan, UT) cells were incubated with the photosensitizer at 1 μg/ml for 18 hours at 2% FBS, after which cells were washed once with phosphate buffered saline and given fresh complete media. After incubation with the photosensitizer, cells were irradiated with the LED illumination setup. Cells were illuminated for 12 hours inside a standard incubator, at 37° C and 5% CO₂, at varying fluence rates (41 nW/cm² to 0.29 mW/cm² for 405nm LEDs, 5.8 μW/cm² to 2.8 mW/cm² for 634 nm LEDs) in order to span the entire dose-response curve for each cell line and condition. An illumination time of 12 hours was chosen to both avoid oxygen depletion and also be representative of the illumination times produced by noninvasive deep light sources.

2.4 Cell viability

Immediately after the conclusion of ALA PDT treatments, cell media was replaced and returned to 10% FBS media. Cells were then incubated under standard conditions for 48 hours. After this regrowth period cell viability was assessed with the WST-1 proliferation assay following the manufacturer's protocol. Treatment groups were normalized to controls in

order to assess their viabilities. Experiments were repeated three times; the data presented herein is the mean and standard deviation of all experiments. Data were fit to Boltzmann curves using the SciDAVis open-source software package [22].

3. Results and discussion

3.1 Fluence dose-response curves

Experiments were carried out for three PDT conditions: 634 nm LED excitation using ALA, 405 nm LED excitation using ALA, and 405 nm LED excitation using TPPS_{2a}. The dose-response curves from these studies using each of the three cell lines are shown in Fig. 2. The LD-50 points calculated from these curves were subsequently used to compare the different treatment conditions and the LD-25 points were used to determine approximate low fluence dose thresholds.

3.2 Blue versus red LED illumination

Given that many noninvasive deep light sources produce light at much shorter wavelengths than traditional light sources, experiments were conducted to determine if there was a benefit from exciting at these shorter wavelengths. It is well known that light alone in the blue region is capable of causing phototoxicity [23]. This blue light toxicity is likely due to cytochrome c, a protein involved in the electron transport chain of cellular respiration, which is known to have strong absorbance in the blue wavelengths due to its heme groups [24]. Experiments were first performed to determine where this effect lies with respect to the PDT regime (Fig. 3). For experiments using 634 nm LED light, no phototoxicity was detected at up to 125 J/cm² (data not shown). When illuminating with 405 nm LEDs, phototoxicity was observed beginning at approximately 1.5 J/cm² as is seen in Fig. 3. This, however, does not overlap with the effects from PDT alone when using ALA, and is orders of magnitude higher than the light levels needed to activate TPPS_{2a}.

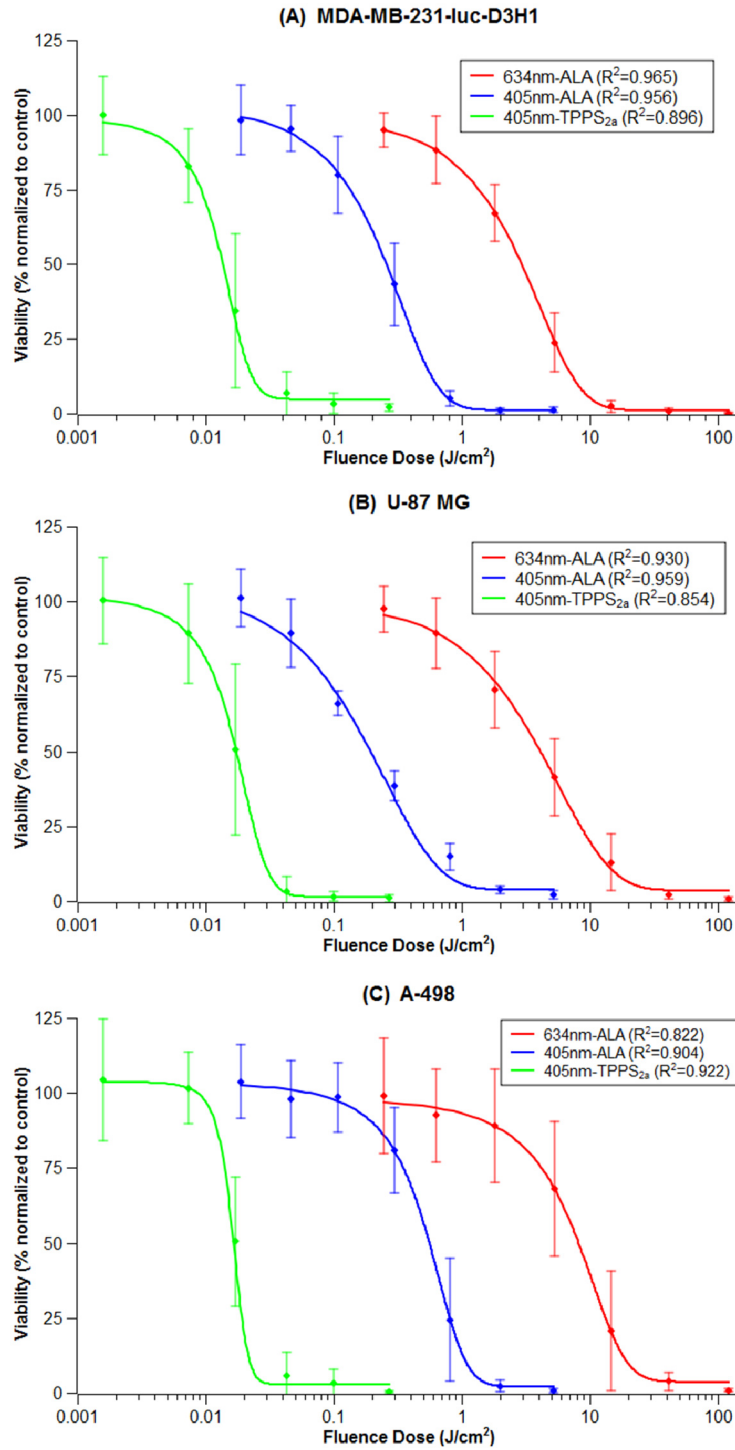


Fig. 2. PDT fluence dose-response curves for MDA-MB-231-luc-D3H1 (a), U-87 MG (b), and A-498 (c) cell lines. Studies using 1 mM ALA and 634nm LEDs are shown in red, 1 mM ALA and 405 nm LEDs in blue, and 1 μ g/ml TPPS_{2a} and 405 nm LEDs in green. Coefficients of determination (R^2) for each fitted curve are included in the legends.

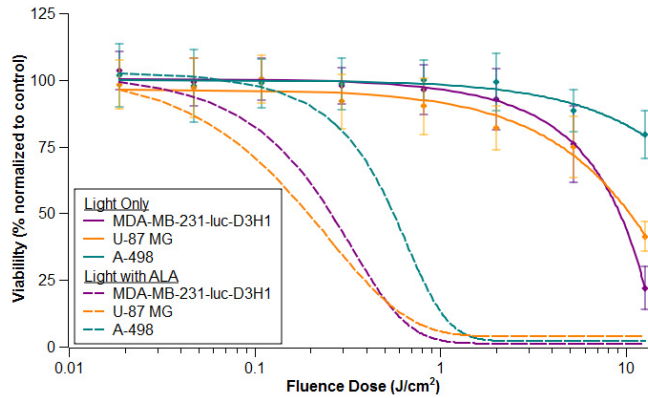


Fig. 3. The comparison of dose response curves between light only (solid lines) and 1 mM ALA PDT (dashed lines) for MDA-MB-231-luc-D3H1 (purple), U-87 MG (teal), and A-498 (orange) cell lines.

In order to quantify the differences between blue and red light PDT excitation, the LD-50 values from each wavelength were compared in Fig. 4. As expected, due to the much stronger Soret-band absorption, the LD-50 measured with 405 nm illumination is on average 15 times less than that obtained with the 634 nm LEDs. The singlet oxygen quantum yields for PpIX and TPPS_{2a} have not been studied using both blue and red light. However, a comparable porphyrin analogue, TPPS, was studied at 424 nm and 630 nm and was found to have similar singlet oxygen quantum yields of 0.69 and 0.58, respectively [25]. This would suggest that there shouldn't be a significant difference in the PDT efficiency for the two light sources when normalized for photon energy and extinction coefficients at the different wavelengths. To validate this, the ratios of the LD-50 values (normalized for photon energy and PpIX extinction coefficient) for blue and red light were calculated (Fig. 4). Although all cell lines match approximately with theory, there are small differences suggesting that some cell lines (notably the U-87 MG) are more susceptible to 405 nm PDT. This could potentially be due to a synergistic effect between the sub-lethal oxidative stress from the blue light phototoxicity and the PDT treatment. Although no intrinsic increase in efficiency appears to exist for blue light, these results highlight and emphasize the significant advantage of blue excitation sources for PDT due to the increased absorption at these wavelengths.

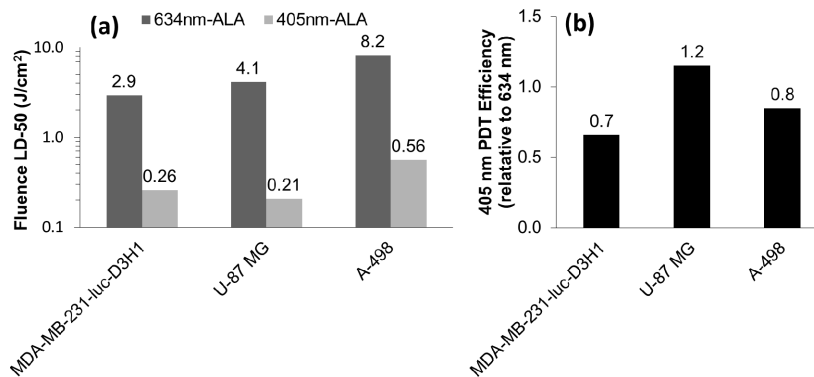


Fig. 4. The comparison of LD-50 values calculated from dose-response curves for each tumor cell line using 405 nm LEDs and 634 nm LEDs (a). The ratios of LD-50 values for 405 nm versus 634 nm LEDs after normalization to wavelength dependent photon energy and PpIX extinction coefficients (b).

3.2 Low fluence dose threshold

In order to determine the low fluence dose thresholds for *in vitro* PDT, the LD-25 values were determined from the TPPS_{2a} dose-response curves of Fig. 2. A comparison across the tumor cells lines can be seen in Fig. 5 below. The average across the cell lines is 12 mJ/cm² and represents an approximate low fluence threshold needed to generate an observable PDT effect. It is important to note however that this serves as a somewhat ideal case given that the excitation wavelength matches well with the peak absorption of these photosensitizers. As an example, the most characterized noninvasive deep light source, Cerenkov luminescence, produces photons over a continuous spectrum inversely proportional to wavelength. Although it might benefit from the ability to cause additional damage with ultraviolet-A light, only a fraction of these photons will be as efficient as those generated from the 405 nm LED source.

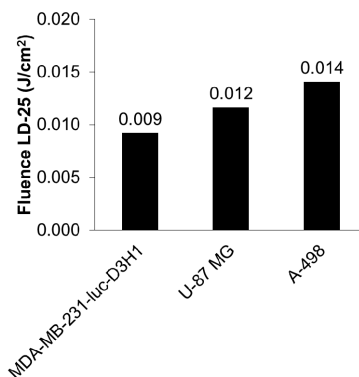


Fig. 5. Low fluence dose thresholds for PDT studies using 1 $\mu\text{g/ml}$ TPPS_{2a} and 405 nm LEDs. Values were calculated using LD-25 points from the fitted dose-response curves for each of the three cell line.

When comparing cell lines across all of the photosensitizer and illumination source conditions tested, the A-498 renal carcinoma cell line was by far the least susceptible to PDT treatments for all conditions. The MDA-MB-231-luc-D3H1 breast tumor cell lines were the most susceptible for treatments using TPPS_{2a} as well as those using 634 nm LED illumination. The U-87 MG glioblastoma cell lines were the most susceptible for ALA treatments using 405 nm LED illumination.

4. Conclusion

This study presented fluence dose-response curves for traditional PDT conditions as well as those for blue light emissions characteristic of emerging noninvasive deep light sources in order to explore the low fluence thresholds of *in vitro* PDT. Presently no illumination setup exists to rapidly generate fluence dose-response curves for *in vitro* PDT treatments. Therefore a novel illumination system for multi-well plate studies, capable of generating dose-response curves from a single plate, was developed. The low profile of the illumination setup allows multiple plates to be simultaneously illuminated inside of a standard cell culture incubator for extended periods of time at a wide range of fluence rates. The flexibility of LED wavelengths to choose from and large dynamic range, spanning from tens of nW/cm² to tens of mW/cm², make it a valuable tool for high throughput multi-wavelength *in vitro* PDT studies.

Low fluence dose thresholds were obtained using the LD-25 values from the 405 nm LED excitation of TPPS_{2a} PDT studies; the average LD-25 across three different cell lines was determined to be 12 mJ/cm². When comparing the efficiency of illuminating with 405 nm versus 634 nm LEDs, the fluence LD-50 values were on average 15 times less when illuminating with blue light. However, when normalized to wavelength dependent photon energy and photosensitizer extinction coefficient their efficiency was very similar, suggesting

that there is no significant difference in reactive oxygen species generation between the two wavelengths on a per absorbed photon basis. Significant differences in susceptibility to PDT existed among the cell lines with the A-498 cells requiring approximately twice the fluence as the other cell lines when using ALA. For TPPS_{2a} studies the renal carcinoma cell line was again the least susceptible to PDT although by a smaller margin. This study firstly demonstrated a dynamic, novel LED system for in vitro PDT studies capable of rapidly generating fluence dose-response curves. Secondly, this system was implemented to ascertain approximate low fluence thresholds to serve as guidance when developing noninvasive deep light sources for ultimate application *in vivo*.

Acknowledgments

This work was supported by the NIH grant R01 EB015471. The authors would like to acknowledge Coherent Inc. for the loan of some of the equipment used in these experiments and Justin Klein for his assistance with the design and construction of the PCBs.